MAGNET SYSTEM OF HEAVY ION SYNCHROTRON AND COOLER RING, TARN II

A. Noda, Y. Hattori, A. Itano†, M. Kanazawa, T.Katayama, M. Kodaira,
M. Mizota, K. Noda, S. Sasaki, N. Takahashi, M. Takanaka, T. Tanabe,
S. Tatsumi, M. Yoshizawa, T. Watanabe and Y. Hirao
Institute for Nuclear Study, University of Tokyo
Tanashi, Tokyo, Japan

Abstract

A heavy ion synchrotron-cooler ring, TARN II is now under construction at Institute for Nuclear Study, University of Tokyo. It can accelerate heavy ion beam with charge to mass ratio of 1/2 up to the energy of 450 MeV/u and the maximum magnetic rigidity is designed at 7 T·m. The focusing structure is based on simple FODO lattice, while the long straight section is designed to have smooth structure of beta and dispersion functions like doublet system.

The main magnet system is composed of 24 dipole and 18 quadrupole magnets. These magnets are fabricated with stacked laminated cores 0.5 mm in thickness with inorganic insulation layers at both surfaces. The dipole magnets with gap height of 80 mm and core length of 1000 mm are made with H-type. The quadrupole magnets with bore radius of 65 mm and core length of 200 mm have hyperbolic pole shape which is smoothly connected to its tangential lines at both sides.

Field properties of all these magnets have already been studied in detail and they are now being aligned to their proper positions with the precision of 0.1 mm, reflecting the results of field measurements from beam dynamical point of view.

Introduction

At INS, the accelerator developments for heavy ion beam have been continued in these ten years. As one of these activities, a storage ring of low energy ion beam called TARN had been operated from August, 1979 to May 1985. Utilizing TARN, a lot of developments for heavy ion acceleration with synchrotron have been performed, for example beam intensity multiplication, beam monitoring of lower intensity, RF system with wide sweep range and ultra-high vacuum technology and so on. Recently stochastic cooling method is applied for low energy (7MeV/u) ion beam, which resulted in reduction of fractional momentum spread from 2 % to 0.06 %. However the dipole magnets of TARN are made of block iron and dynamical acceleration studies had been left for further development. In addition, needs for electron cooling system, which is expected to attain much better energy resolution than stochastic method, have been increasing to pursue precise experiments for nuclear and atomic physics and the length of 1.8 m of the long straight section at TARN was felt too short for installation of electron cooling devices.

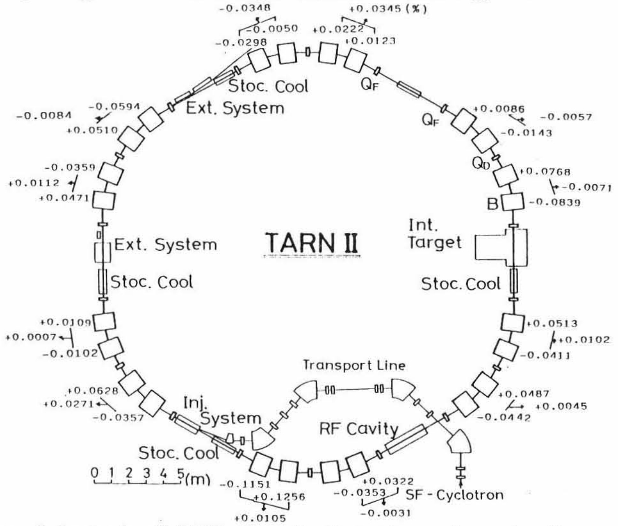

Fig. 1 Layout of TARN II. Each number given to the dipole magnet represents its relative deviation of deflection angle (%).

From the above situation, construction of TARN II is started from the begining of 1984. As the injector, the SF cyclotron at INS with K-number 67 is to be used. The average radius of TARN II is determined at 12.376 m, because the circumference of TARN II should be integral multiple (in the present case 17 times) of that of outermost orbit of the cyclotron in order to assure overlapping condition of microscopic bunches of the beam from the cyclotron during injection process. In Fig. 1, layout of TARN II is shown. In the present paper, lattice and magnet design is described at first and the results of magnetic field measurements are presented together with their reflection on final magnet arrangement.

Lattice Design

The focusing structure of TARN II ring is designed based on a simple FODO lattice because of its compactness so as to realize the higher maximum energy in rather limited site. Long straight sections are made by inserting drift spaces 4.25 m in length between horizontally focusing quadrupole magnets at every unit cell and the unit cell coincides with the superperiod. The whole circumference is composed of six unit cells. For usual synchrotron acceleration, these cells are all excited identically resulting regular structure of Twiss parameters and dispersion function with small maximum β-values as shown in Fig. 2, which is preferable from the point of view of increasing machine acceptance (Synchrotron Mode). The rather higher

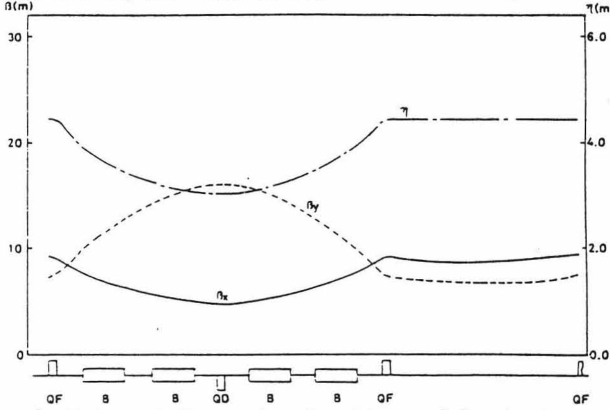

Fig. 2 Beta and dispersion functions of Synchrotron Mode of TARN II.

---

† National Institute of Radiological Sciences, Anagawa, Chiba 260, Japan.

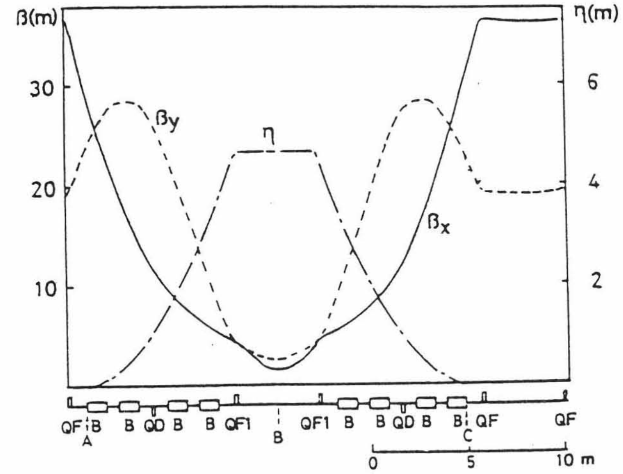

Fig. 3 Beta and dispersion functions of TARN II Cooler Ring Mode. One third of the circumference is shown in the figure.

superperiodicity of six is also beneficial to avoid sector resonances in choosing the working line. However for this excitation mode, every long straight section has finite dispersion as large as ∿5 m, which seems to be unsuitable for momentum cooling because transverse emittance blow up is anticipated during momentum correction process.

So as to realize doubly achromatic section required for momentum cooling equipment together with finite dispersion section needed for internal target position, superperiodicity of the lattice is reduced to three by changing only excitation pattern of quadrupole magnets keeping the operating point at the same position of (1.75, 1.25) (Cooler Ring Mode). By making the arrangement of magnets of mirror symmetry with respect to point B in Fig. 3 and imposing some condition on the field gradient of QF1, the straight section just outside of points A and C is made to be doubly achromatic[1].

From the point of view of sector resonance, it is preferable to avoid acceleration by Cooler Ring Mode with superperiodicity of 3. As Cooler Ring Mode is found to be transferable with Synchrotron Mode, such operation as uses Synchrotron Mode for beam injection, RF acceleration and betatron pre-cooling with stochastic method and then move to Cooler Ring Mode for electron beam cooling is proposed[1]. With this method, beam intensity usable for electron cooling is expected to be increased by factor of several times.

Magnet Design

Main magnet system of TARN II ring consists of 24 dipole and 18 quadrupole magnets. Assuming the beam emittances after multi-turn injection to be 400π and 10π mm·mrad in horizontal and vertical directions, respectively and fractional momentum spread of ±0.22 %, required useful apertures for the case of Synchrotron Mode are estimated at 200 x 50 mm^2 and 185 x 60 mm^2 (Hori. x Vert.) for dipole and quadrupole magnets, respectively. Reflecting the fact that maximum values of beta functions are larger for Cooler Ring Mode, the horizontal beam emittance after multi-turn injection should be limited below 70π mm·mrad. The vertical useful aperture is enlarged to 60 mm also for dipole magnets considering the case where Cooler Ring Mode is applied from the begining without pre-cooling. So the magnet gap is chosen at 80 mm taking into account additional spaces necessary for vacuum chamber wall and heat insulator material for baking process to attain ultra-high ($\sim 10^{-11}$ Torr) vacuum.

As the ring is AC operated with repetition rate of 1/2 Hz for Synchrotron Mode and dB/dt amounts to 2.3 T/sec. for dipole magnet, the magnets should be made of stacked laminated steel so as to suppress the effect of eddy currents. Quadrupole magnets in old TARN are made of laminated cores 0.5 mm in thickness and they are used as the focusing elements of TARN II. Six quadrupole magnets are newly fabricated to hold sixfold symmetry. Its bore raius is 65 mm and the pole shape is hyperbola smoothly connected to its tangential lines at both sides. Pole width is determined at 150 mm. The pole profile of the quadrupole magnet is shown in Fig. 4. End cut shaping of four steps is applied to pole end to increase the flat region of effective length of the quadrupole magnet[2].

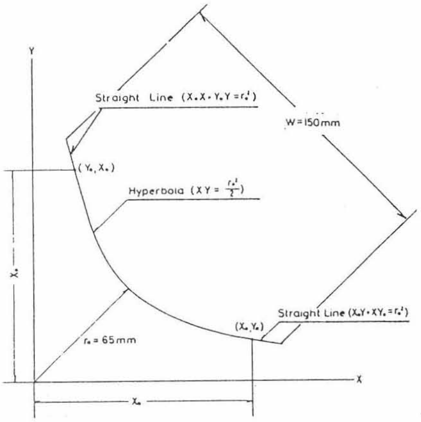

Fig. 4 Pole profile of the quadrupole magnet of TARN II.

H-type is adopted for the type of the dipole magnets newly made, because of its good symmetry and merit of coil location preferable for AC operation[1]. The dipole magnet is decided to be made by straight shape because of its easiness of fabrication and flexibility for further conversion to a larger ring. Its length is suppressed at rather shorter value (1 m) to reduce the sagitta at reasonable value (16.4 mm). The pole edges are shaped with B constant curve[3] to realize the uniform field in the wide region of ±100 mm in radial direction and for wide range of excitation level up to 18 kG. Small shims connected smoothly to the B constant curve at both sides as shown in Fig. 5 are attached so as to modify the field structure which tends to fall down at both sides due to saturation of iron at higher fields. The shape of the shim is determined based on the numerical calculation with use of the computer code TRIM[4]. Rogowsi's end cut shaping[5] is applied at both ends of the magnet with approximation of three steps so as to suppress the variation of the effective field boundary depending on the excitation level.

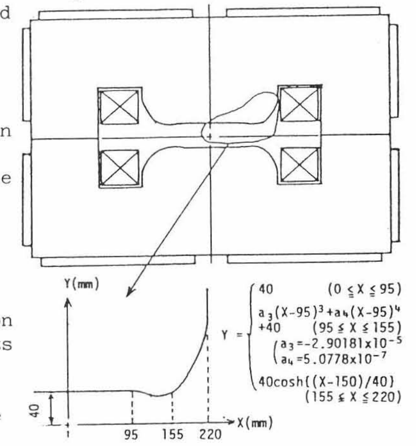

$$Y = \begin{cases} 40 & (0 \leqq X \leqq 95) \\ a_3(X-95)^3 + a_4(X-95)^4 + 40 & (95 \leqq X \leqq 155) \\ \quad \left(\begin{array}{l} a_3 = -2.90181 \times 10^{-5} \\ a_4 = 5.0778 \times 10^{-7} \end{array} \right. & \\ 40\cosh\{(X-150)/40\} & (155 \leqq X \leqq 220) \end{cases}$$

Fig. 5 Cross sectional view of dipole magnet of TARN II.

As the material of the laminated core, cold rolled silicon steel strip (S23 in Japanese Industrial Standard) with special heat treatment is adopted. It is 0.5 mm in thickness and surface coated by an inorganic insulation layer.

Field Measurement of Magnet

Dipole Magnet

The static field structure of the dipole magnet has been studied with a DC power supply which can excite the single dipole magnet up to the maximum current of 4000 A. The absolute value of the gap field is measured with use of proton resonance at the center of the magnet. In Fig. 6, measured excitation characteristics of the dipole magnet is given together with that of computer calculation by TRIM. It is found that saturation effect of the iron core begins to appear around 15 kG and for the excitation current of 3500 A, 19 kG is obtained. The reason why real saturation effect is somewhat smaller compared with that of computer calculation is considered to be due to the fact that calculation assumes lower side B-H characteristics and rather smaller packing factor for safety. The difference of absolute field strength from magnet to magnet when they are excited by series connection is also obtained from this measurement.

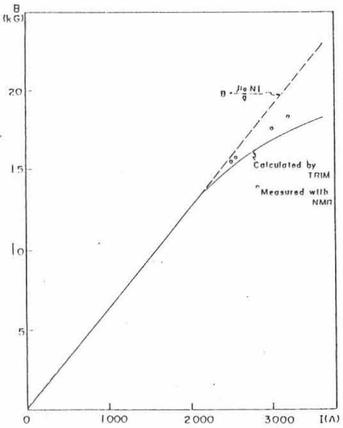

Fig. 6 Excitation curve of dipole magnet for TARN II.

For the measurements of radial field distribution and effective field length, a flip coil system is fabricated. The field strength is measured by rotating the coil set up in horizontal plane precisely 180° with use of a stepping motor of 0.36° step. The induced voltage is integrated by a simple integrator utilizing ultra-low offset drift (0.2 μV/°C) operational amplifier, which is measured by a high precision digital voltmeter. The integrator is reset by the timing signal which triggers the coil rotation and the digital voltmeter is externally triggered by the signal of the rotation end. The integration is applied for rotations both clockwise and counter clockwise and these values with oposite polarity are subtracted. By this procedure the offset drift is cancelled if it does not change in a short time during these succesive rotations. The precision of the measurement is found better than ± 5 x 10^{-5} even for the lowest excitation current. The coil position can be controlled in radial direction by driving mechanisms attached to the both ends of the container rod made of epoxy glass and above measurement is applied at various radial positions automatically. In Fig. 7, the flip coil system attached to the dipole magnet is shown.

The effective length of the dipole magnet is measured by a small coil with the dimension of 10 x 10 mm^2, which can slide along the epoxy glass rod automatically by a driving mechanism using a pulse motor. The position of the coil is moved 10 mm step in the direction of the magnet axis and the field strength is measured by coil flip. These values are integrated along the magnet axis and divided by the center value. Thus the effective length of sharp edge model is obtained. Combining this with the result of absolute value measurement by NMR above mentioned, the deviation of the integrated field strength along the magnet axis $(\Delta B\ell/B\ell)$ is obtained. In Fig. 8, a typical result is shown for the excitation current of 1500 A. Deviation among the magnets is less than ± 0.13 % and by making a pair with the similar size deviation of opposite polarity for the adjacent two dipole magnets as shown in Fig. 1, the closed orbit distortion (C.O.D.) is expected to be suppressed. In reality, C.O.D. is found to be suppressed less than 9 mm by a computer calculation even for the injection field level, while the assumed C.O.D. for aperture requirement is 16.4 mm.

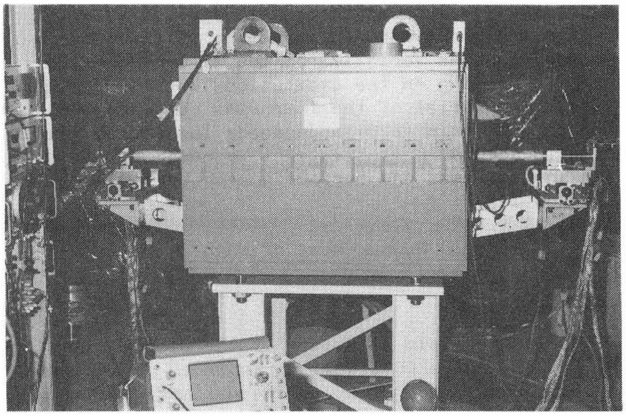

Fig. 7 A flip coil system attached to the dipole magnet for TARN II.

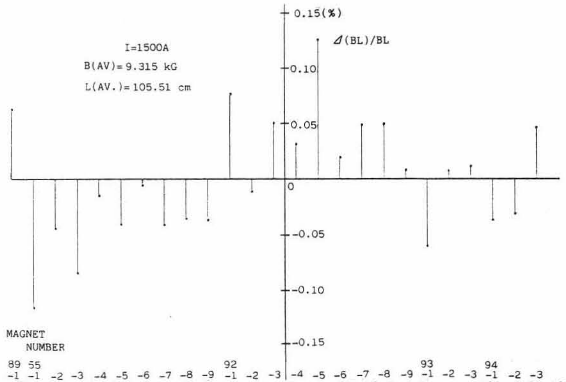

Fig. 8 Deviation of integrated field strength of the dipole magnets for TARN II.

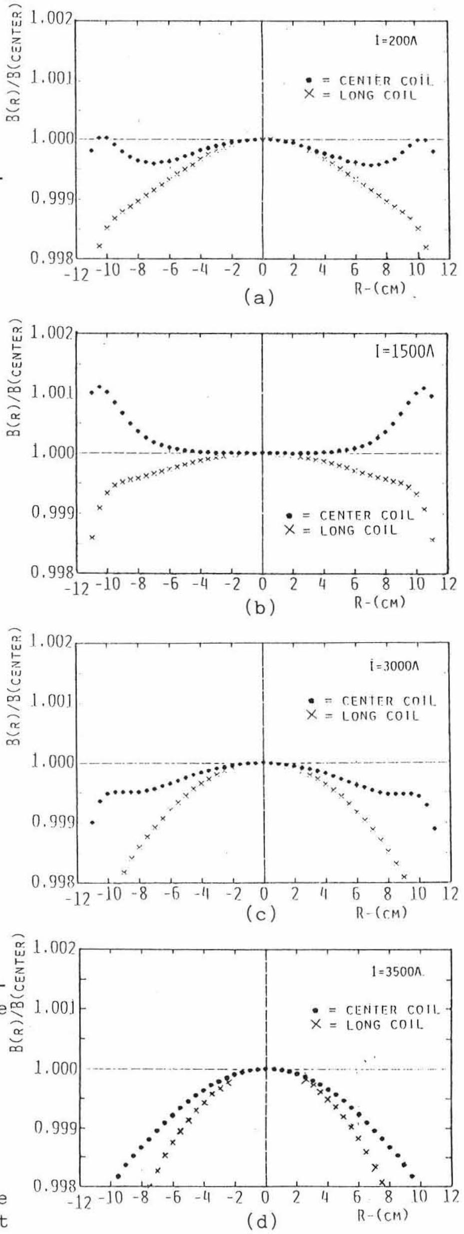

Fig. 9 Radial distributions of field strength (center coil) and integrated field strength (long coil) of the dipole magnet for the excitation currents of (a)200 A, (b)1500 A, (c)3000 A and (d)3500 A.

Radial distributions of the field strength at the center of the magnet and integrated field strength, $\int B(x,s)ds$, are measured by two coils with dimensions of

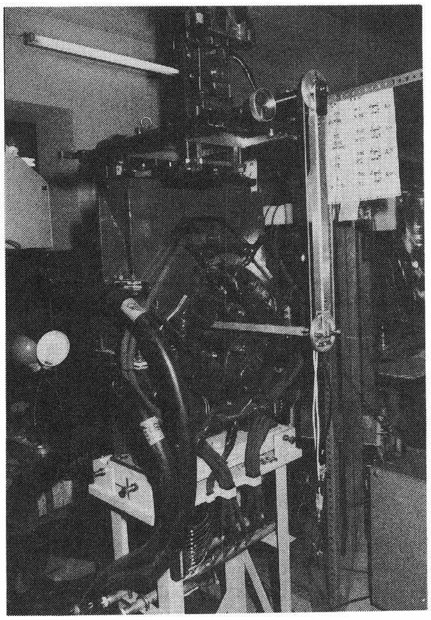

Fig. 10 A translation coil system attached to the quadrupole magnet for TARN II.

100 x 10 mm^2 and 1600 x 20 mm^2, respectively. These coils are fixed in a epoxy glass rod and the shorter coil is located at the center of the rod. Typical results of the measurements are shown in Fig. 9 for the excitation currents of 200, 1500, 3000 and 3500 A, corresponding to the field levels of 1.25, 9.3, 17.4 and 19 kG, respectively. It is seen that saturation effect of the iron core enlarges sextupole component at the higher excitation levels above 3000 A. Measured radial distributions are fitted by a polynomial expansion and multipole components are derived. The sextupole component is evaluated to be less than 0.3 $1/m^2$ for the excitation currents below 3000 A and it increases up to 0.5 $1/m^2$ for the excitation current of 3500 A. Using the sextupole component of each magnet and assuming the arrangement of the dipole magnets to reduce C.O.D. above mentioned, the stopband of the nearby third order resonance ($3\nu_H = 5$) is estimated. The excitation coefficient[6] of the resonance are calculated at 5 x 10^{-4} and 1.6 x 10^{-3} for Synchrotron Mode and Cooler Ring Mode, respectively if only sextupole components in the dipoles are included.

Quadrupole Magnet

The field gradient of the quadrupole magnet is measured by a translation coils. Two coils of the same dimension (6.4 x 30 mm^2) with 10 mm distance are translated in a horizontal plane and the difference of the induced voltages at these coils is measured. From this value, the derivative of the field gradient at the place is directly obtained. Derivative of the integrated field gradient along the magnet axis is also measured by twin coils with larger dimension (8 x 774 mm^2) at the same time, because these two kinds of twin coils are installed in a single coil assembly. In Fig. 10, the measurement system by twin coils attached to the quadrupole magnet is shown. The radial distributions of the field gradient and its integrated value along the magnet axis are shown in Fig. 11 for the excitation currents of 6 and 35 A as a typical example. The measurement is executed for the field levels from 1 to 70 kG/m. The measured radial distribution of the derivative of the field gradient is fitted by a polynomial expansion and higher multipole components from sextupole are derived. By integration of this polynomial, radial distribution of the field gradient is obtained. The observed sextupole components among all the magnets are less than 3 x 10^{-2} $(1/m^2)$ even for the excitation level of 1 kG/m. The allocation of the quadrupole magnets is determined to reduce the excitation coefficient of the resonance $3\nu_H = 5$ using the measured sextupole components. By such arrangement of the quadrupole magnets, the excitation coefficient of the resonance is reduced to 1.3 x 10^{-3} for Cooler Ring Mode even for the injection excitation level. The corresponding stopband is estimated at 0.0008 assuming beam emittances of 200π and 15π mm·mrad for horizontal and vertical directions, respectively, which is well in a tolerable size.

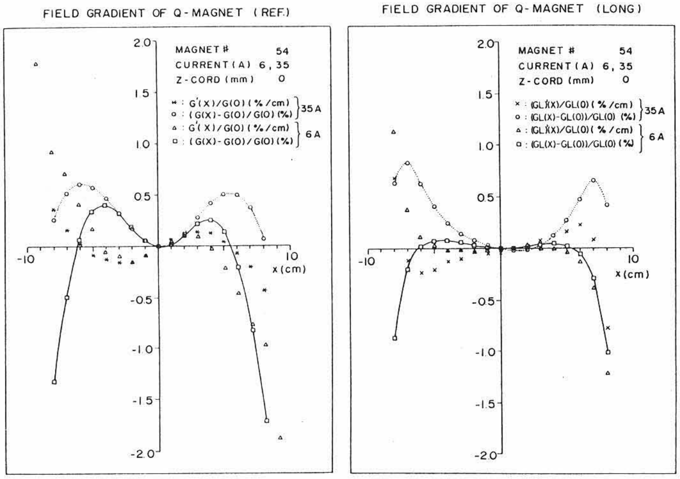

(a) (b)

Fig. 11 Radial distributions of field gradient (a) and integrated field gradient along the magnet axis (b) of the quadrupole magnet for TARN II for the excitation currents of 6 and 35 A.

Alignment of Magnets

Allocation of the dipole and quadrupole magnets are determined taking the field properties into account as mentioned above. They are now being aligned to their precise positions. Utilizing two standard holes attached to each magnet, whose positions with respect to pole shape are precisely adjusted, the distances between magnets and center pillar are measured. These distances are measured with Invar wire 1.65 mm in diameter pulled with 8 kg tension from both ends. Although the thermal expansion coefficient of Invar is one order smaller compared with usual iron, absolute length of the wire is calibrated with laser deflectmeter on a standard bench before and after each measurement. With this procedure, systematic error due to change of wire length can be eliminated. Precision of a few ten μm is attained for the measurement of distances between magnets and center pillar.

Ackowledgement

The authors would like to express their sincere thanks to other members of Accelerator Research Division of Institute for Nuclear Study, University of Tokyo for their collaboration thoughout field measurement of the dipole magnets. Orbit calculation with SYNCH, field calculation with TRIM and analysis of obtained data from field measurement are performed with M380R at INS.

References

(1) A. Noda et al., IEEE Trans. on Nucl. Sci. NS-32, No. 5 (1985) 2684.
(2) A. Noda et al., INS-NUMA-23 (1980).
(3) H. Kumagai, Nucl. Instr. Meth. 6 (1960) 213.
(4) A. M. Winslow, UCRL-7784 (1964).
(5) W. Rogowski, Archiv für Electrotechnik 7 (1923) 1.
(6) G. Guignard, CERN 78-11 (1978).